Published in final edited form as:
Hippocampus. 2004 ; 14(2): 255–264. doi:10.1002/hipo.10172.

Expression of Long-Term Potentiation in Aged Rats Involves Perforated Synapses But Dendritic Spine Branching Results From High-Frequency Stimulation Alone

Tiruchinapalli M. Dhanrajan[1], **Marina A. Lynch**[2], **Aine Kelly**[2], **Victor I. Popov**[1,3], **Dmitri A. Rusakov**[1,4], and **Michael G. Stewart**[1,*]

[1] Department of Biological Sciences, The Open University, Milton Keynes, United Kingdom [2] Department of Physiology, Trinity College, Dublin, Ireland [3] Institute of Cell Biophysics, Russian Academy of Sciences, Pushchino, Russia [4] Institute of Neurology, University College London, London, United Kingdom

Abstract

Evidence for morphological substrates of long-term changes in synaptic efficacy is controversial, partly because it is difficult to employ an unambiguous control. We have used a high-frequency stimulation protocol in vivo to induce long-term potentiation (LTP) in the hippocampal dentate gyrus of aged (22-month-old) rats and have found a clear distinction between animals that sustain LTP and those that fail to sustain it. The "failure group" was used as a specific/"like-with-like" control for morphological changes associated with the expression of LTP per se. Quantitative optical and electron microscopy was used to analyze large populations of dendritic spines and excitatory perforant path synapses; LTP was found to be associated with an increase in numbers of segmented (perforated) postsynaptic densities in spine synapses. In contrast, an increase in the number of branched spines appears to result from high-frequency stimulation alone. These data shed light on the current controversy about the expression mechanism of LTP.

Keywords

perforated synapses; branched spines; LTP

INTRODUCTION

Since the early 1970s, long-term potentiation (LTP) of synaptic transmission in the hippocampus (Bliss and Lomo, 1973) has been used widely to study the basic mechanisms believed to underlie memory formation (Bliss and Collingridge, 1993). A number of studies have shown links between LTP and memory formation. Xu et al. (1998) demonstrated that spatial exploration induced a persistent reversal of LTP in rat hippocampus, while Moser et al. (1998) reported that spatial learning was impaired after saturation of LTP. Fear conditioning was shown to occlude LTP-induced presynaptic enhancement of synaptic transmission in the cortical pathway to the lateral amygdala (Tsvetkov et al., 2002), and Bozon et al. (2002) demonstrated that the gene Zif268 plays a critical role both in initial triggering of the genetic machinery for maintenance of the later phases of LTP, and also in

[*]Correspondence to: Michael. G. Stewart, Department of Biological Sciences, The Open University, Milton Keynes, MK7 6AA, UK. m.g.stewart@open.ac.uk.

Europe PMC Funders Author Manuscripts

spatial memory formation. The suggestion that LTP meets one of the principal criteria for long-term memory storage was made recently by Abraham et al. (2002), who demonstrated that stable long-lasting LTP can be disrupted by exposure of rats to an enriched environment.

Because consolidation of long-term memories is believed to involve structural changes, morphological correlates of LTP have been investigated intensively with a variety of preparations, most frequently from rat, using acute slices in vitro (Chang and Greenough, 1984), organotypic hippocampal culture (Muller et al., 2000), and stimulation in vivo (Desmond and Levy, 1986, 1988, 1990; Geinisman et al., 1991, 1994; Rusakov et al., 1997; Stewart et al., 2000; Weeks et al., 2000, 2001). While the finding that LTP is associated with an increased number of segmented perforated synapses appears to be unchallenged (Geinisman et al., 1996), disagreement continues as to whether LTP results in the formation of new synapses.

A confocal imaging study by Hosokawa et al. (1995) showed only subtle changes in morphology of living dendritic spines after LTP induction, but a reduction in spine densities was shown 24 h after LTP induction in vivo (Rusakov et al., 1995). Real-time imaging data using in vitro preparations, however, demonstrated rapid morphological changes (Engert and Bonhoeffer, 1999; Maletic-Savatic et al., 1999; Toni et al., 1999, 2001) 1–2 h after LTP induction. In contrast, studies with acute slices showed a remarkable stability of synapse density in potentiated tissue (Sorra and Harris, 1998), and three-dimensional (3D) reconstruction data argued against rapid formation of functional synapses on branched spines (Fiala et al., 2002). In cultured hippocampal neurons, both pruning and formation of spines occur (Goldin et al., 2001), and spines can actually retract after back-propagating action potentials (Korkotian and Segal, 2001).

Taken together, however, these findings do not show convergence of agreement on structural correlates of LTP induction. Interestingly, comparison of physiological protocols shows that while many investigators use similar methods for LTP induction, the choice of control varies, even though it is critical to ensure that an observed structural change is specific to the enhancement of synaptic transmission. The most common form of LTP is N-methyl-D-aspartate (NMDA) receptor-dependent; thus, blockade of NMDA receptors allows the same stimulation protocol without induction of LTP. However, both normal functioning of NMDA receptors and Ca^{2+} homeostasis are intimately involved in morphogenic mechanisms inherent in nerve cells, whether or not morphogenesis is associated with LTP (Murase et al., 2002; Nimchinsky et al., 2002). Consequently, suppressing these mechanisms could suppress morphogenesis triggered by the LTP induction protocol. Moreover, Weeks et al. (2003) have shown that while most changes observed after the induction of LTP in vivo are LTP-specific, and not simply the result of tetanic stimulation, blockade of NMDA receptors alone can induce structural changes, including a decrease in the length of perforations in concave perforated synapses, a reduction in the number of convex perforated synapses, and an increase in synaptic length compared with controls.

To overcome these difficulties, one would ideally prefer identical induction protocols, physiological conditions, and pharmacological manipulations across all animals. However, is such an approach feasible? In fact, LTP induction does not always achieve 100% success, a rate that reduces sharply with age (deToledo-Morrell et al., 1988; Barnes et al., 2000; Stephan et al., 2002). This gave us the opportunity to use aged animals and select test and control groups on the basis of successful, or unsuccessful LTP induction, with all other conditions identical. Unbiased stereological techniques were then employed to analyze large numbers of synapses and dendritic spines in these groups. Our data show that high-frequency stimulation alone produces a dramatic increase in numbers of branched spines,

but not synapses, whereas LTP is specifically associated with an increased number of segmented synapses with perforated active zones.

MATERIALS AND METHODS

Induction of LTP

All electrophysiological experiments were conducted in the Department of Physiology at Trinity College, Dublin. To ensure unbiased morphological analysis, animals were coded and the codes were not released until all the data were acquired and ready for statistical analysis.

Aged male Wistar rats (~22 months) were anesthetized with urethane, secured in a stereotactic frame with recording and stimulating electrodes placed in the dentate gyrus and perforant path of the right hemisphere, as described previously (McGahon and Lynch, 1996). Test shocks (1/30 s) were delivered unilaterally for 10 min before and 45 min after tetanic stimulation (three trains of high-frequency stimulation; 250 Hz for 200 ms; intertrain interval 30 s). At the end of the recording period, animals were perfused transcardially with a phosphate-buffered solution (PBS, 0.1 M) of 2% glutaraldehyde and 2% paraformaldehyde at pH 7.4, and brains were removed from the rats and kept overnight in the same fixative. After coding, the brains were transferred to The Open University, United Kingdom, where the hippocampus was dissected and four 1-mm slabs were taken from the septohippocampal axis of each hemisphere of each animal. Two of these slabs were processed for rapid Golgi staining, and two were processed for electron microscopy. Golgi impregnation was carried out using a modified rapid Golgi protocol (Fairen et al., 1977; Patel and Stewart, 1988); serial sections perpendicular to the septotemporal axis (~80 μm thick) were then cut using a tissue chopper. The sections were dehydrated in graded series of alcohol and embedded with DPX mountant on a glass slide.

Tissue sections for electron microscopy were collected into (0.1 M) phosphate buffer for epoxy resin processing. The sections were postfixed in 0.1% (w/v) osmium tetroxide (Sigma Chemical Co. Ltd, UK) in 0.1 M phosphate buffer for 1 h and were then dehydrated and flat embedded in epoxy resin (Agar 100; Agar Scientific, UK). The resin block with the tissue was allowed to polymerize for 48 h at 60°C. Excess resin was trimmed away, and semithin serial sections were cut using a Leica ultra microtome and stained with 0.1% toluidine blue (Sigma, UK), in order to observe the granule cell layer. Serial ultrathin sections of silver-gold interference color (80 nm) were cut and collected in pairs of two on carbon-coated slot grids (2 × 1 mm; Agar Scientific, UK) and stained using uranyl acetate (5% w/v distilled water) and lead citrate (0.3% w/v in 0.1 M sodium hydroxide). Finally, the sections were examined in a JEOL 1010 electron microscope at an accelerating voltage of 80 kV. Digital images from serial sections of the middle molecular layer of the dentate gyrus were acquired using a Kodak Megaplus CCD camera attached to the microscope.

Quantification of Dendritic Spines Using Image Analysis and Tilting Disector Technique

A semiautomated image analysis technique was used for quantification of dendritic spines. This method is based on skeletonized images of dendritic profiles and allows quantification of large populations of dendritic fragments acquired using a CCD camera mounted on a Nikon Microscope (for technical details, see Rusakov et al., 1995, 1997). One dendritic fragment is illustrated as an original image (Fig. 1C) and one with a superimposed skeleton (Fig. 1E); another dendritic fragment is illustrated with the generated profile image (Fig. 1D) and an overlap of the original and skeletonized image (Fig. 1F). Two parameters, spine length and inter-spine distances along a dendrite, were acquired and assessed using this procedure. An unbiased stereological technique, the “tilting disector,” was used to assess the

true (3D) numerical density of spines along the dendrites (Rusakov et al., 1995). This technique uses the same principle as the disector technique (Sterio, 1984; Gundersen, 1986) and is based on counting spines profiles that are present at one angular position of the dendrite but are not present in the other angular position (Fig. 5 in Rusakov et al., 1997). The only assumption required in estimating the true spine density along the dendrites is that the distribution of spines around the longitudinal axis of a dendritic stem is uniform, which is very likely in most cases. The total number of spines n, which are scored within a sector of β degrees around the dendrite axis, will therefore give the estimated total number of spines (i.e., within a "sector" of 360°) N:

$$N=360n/\beta$$

These counts, carried out for a representative group of dendrites, generate a stereological correction factor for the dendritic population of interest. For the dentate granule cell dendrites, this factor was determined in our previous study as 1.62 (Rusakov et al., 1997). This implies that the numbers of spines counted in profile images have to be multiplied by 1.62 to obtain a stereological estimate of total (3D) spine numbers/ densities along dendrites.

Quantification of Synapses Using the Disector Technique

Synapses can vary in shape and can be classified as curved, segmented, or perforated, and the probability of any given synapse appearing in a plane more than once is high, leading to difficulties in deciding whether they belong to a single synapse. Unbiased stereological techniques, such as the "double disector" (Sterio, 1984) and the "fractionator" (Gundersen, 1986), help overcome these problems. The mean synapse density N_{Vsyn} was calculated as:

$$N_{Vsyn}=\sum N_{syn}/tA$$

where t is the thickness, A is the sampling frame area (35 μm^2) and (N_{syn}) is the number synapses that appear in the counting frame of one slice (the reference), but not on the adjacent section (the lookup). A grating replica (2,160 lines/mm) was used for calibration purposes.

From each aged rat, 24 serial ultrathin disector images were acquired from the left and right hemispheres. Electron micrographs were taken at a magnification of ×8000 and stored digitally on magneto-optical discs. The synapse density (N_{Vsyn}, calculated in μm^3) was estimated without discrimination between individual synaptic types. Regardless of whether they were spine or shaft synapses, 90% of the total visible synapses comprised asymmetric synapses.

3D Reconstruction From Serial Ultrathin Sections

Serial sections of gray-white color (60 –70 nm), 50 – 80 μm from granular cell bodies were collected on Pioloform-coated slot grids and counterstained with saturated ethanolic uranyl acetate, followed by Reynolds lead citrate, and were then placed in a rotating grid holder to obtain uniform orientation of sections on adjacent grids. Sections were photographed at ×6000, in a JEOL 1010 electron microscope. Digitally scanned electron micrograph negatives with a resolution of 900 dpi were aligned as JPEG images using IGL Alignment and Trace software developed by Dr. J. Fiala and Dr. K. Harris (http://synapses.bu.edu). Alignments were done for full-field images Contours of individual dendrites, axons, dendritic spines, postsynaptic density (PSD), and mitochondria were traced digitally and a segment of dendrite was reconstructed.

Statistical Analysis

The unbiased estimation of interhemispheric alterations in spine density, spine length, branched spines, synapse density, spine synapses, and perforated synapses in the middle molecular layer of the dentate gyrus was studied using analysis of variance (ANOVA; Statistica); pairwise comparison was made using *t*-tests. Significance was taken at $P < 0.05$.

RESULTS

LTP Induction

High-frequency stimulation of the perforant path was applied to the right hemisphere of eight aged rats (Fig. 1A). Four rats exhibited potentiation of the synaptic response that was ≥20% above the pre-tetanus level, while four aged rats did not sustain LTP. As the entorhinal cortex-dentate granule (EC-DG) system is largely unilateral (Steward and Vinsant, 1983), the left hemisphere of each animal served as its own control. The population excitatory postsynaptic potential (EPSP) slopes obtained for each aged animal were recorded and mean values computed; for comparison, mean EPSP slopes are shown for six 4-month-old rats. These are similar to those of the four aged rats that exhibited LTP (Fig. 1A).

Spine Density and Spine Length

Morphological changes in dendritic spines and synapses were quantified in the middle molecular layer of the dentate gyrus. A characteristic section of Golgi-impregnated dentate gyrus containing three granule cell bodies and their dendritic arborizations is shown in Figure 1B. A representative dendritic fragment is shown in Figure 1C and a thresholded image of this fragment is shown in Figure 1D. Figure 1E shows a line skeleton from the thresholded image with the dendrite and spines, and Figure 1F shows a line skeletonized image of another dendrite fragment. Lengths of spines are computed from these skeletonized images, from the center of the dendrite. Figure 1G shows a high-magnification image of a fragment of dendrite with a branched spine (asterisk) that appears blurred as it is just out of the plane of vision. Figure 1H shows an example of another small dendrite fragment with a branched spine (asterisk), on this occasion clearly visible in the plane of vision. 9,302 spines from Golgi impregnated tissue were examined in this study: 1,983 spines in the stimulated hemisphere of aged rats that did not potentiate, and 2,511 spines in the control hemisphere of these rats; while 2,249 were in the stimulated hemisphere of the aged rats that did potentiate and 2,559 in the control hemisphere.

To assess qualitatively whether such counts in Golgi preparations were compatible with the precise data provided by 3D reconstructions from serial ultrathin sections, we reconstructed one dendritic fragment in the middle molecular layer of the dentate gyrus, ~100 μm from the granule cell layer, in a stimulated rat that showed sustained LTP. The selection of this fragment was arbitrary (as it is not possible to choose between dendrites in ultrathin sections) and its reconstruction is illustrated in Figure 2A–C. This fragment contained 30 spines, two of which accommodated two PSDs on two separate branches. To make a visual comparison with the typical profile images of dendrites of the same order seen in Golgi preparations, we rotated the reconstructed fragment along its longitudinal axis and recorded its profile image at each rotation angle. These profiles are depicted in Figure 2A and appear consistent with Golgi profiles shown in Figure 1C–F. Nine ultrathin sections from the series of 150 sections, which comprised the reconstruction, are shown in Figure 2B (labeled 42–50); the dendrite is shown in rotation in Figure 2C (II), with the mitochondria (blue) appearing in filamentous form, and in Figure 2C (III) with only the external skin of the reconstruction. Spines with PSDs (red) are shown in Figure 2C (I–IV), with an example of bifurcating spines (Sp1 and Sp2) on Figure 2C (I). The branched spines are outlined in the box in Figure 2C (III) and are shown at high magnification in Figure 2C (IV).

Table 1 presents mean values for spine density and length in the hippocampus prepared from two groups of rats: aged potentiated and sustaining LTP, and aged but nonpotentiated (failing to sustain LTP). There were no significant differences between spine density in the stimulated hemisphere of rats that sustained LTP and the unstimulated hemisphere (0.96+0.09 and 0.95+0.12 spines/μm, respectively). Mean spine density was slightly lower (by 18%) in the stimulated hemispheres of aged rats that sustained LTP (0.95 spines/μm) compared whose that failed to sustain LTP (1.13 spines/μm). Mean spine length was slightly greater (16%) in the stimulated hemisphere of aged rats that sustained LTP (0.94 μm^{-1}), compared with the stimulated hemisphere of aged rats that did not sustain LTP (0.812 μm^{-1}); however, none of these differences was significant.

Branched Spines

A twofold increase in the percentage of branched spines was observed in the stimulated hemisphere after 45 min (Table 1), whether or not the rats sustained LTP. The percentage of branched spines increased from 3.94% to 6.57% of the total spine number in the stimulated, compared with the unstimulated hemisphere of aged rats that sustained LTP ($P < 0.02$); the corresponding increase in aged rats that did not sustain LTP was from 2.53 to 6.37% ($P < 0.02$). Interestingly, the percentage of branched spines from the 3D reconstruction sample taken from a stimulated rat that sustained potentiation was 6.7%.

Synapse Density

The mean densities of synapses—spine, shaft, and total—are presented in Table 1. Mean values for total synapse density were 1.497 per μm^3 ($P < 0.88$) and 1.46 per μm^3 ($P < 0.42$) in the stimulated, compared with the unstimulated, hemisphere of rats that sustained LTP and did not sustain LTP, respectively. These changes represented decreases in synapse density of 25% and 22% in the stimulated, compared with unstimulated, hemispheres of rats that sustained, and did not sustain, LTP respectively. These differences did not reach statistical significance and, similarly, analysis of the data obtained for axospinous synapses (the great majority in the molecular layer) failed to show any statistically significant changes (Table 1). In the control hemisphere of potentiated rats synapse density was 1.67 per μm^3, while in the potentiated hemisphere the values fell to 1.31 per μm^3, and in contrast in the rats that failed to sustain potentiation synapse density was 1.48 per μm^3 in the stimulated hemisphere and 1.24 per μm^3 in the unstimulated hemisphere. No significant differences were seen in synapse densities for shaft synapses whether between hemispheres of rats that had potentiated, or those that failed to sustain potentiation.

Postsynaptic Density Measurements

The branched spines shown in the reconstruction in Figure 2C are contacted by macular synapses (unperforated PSDs), and the thin sections in Figure 2 (42–50) show several unperforated PSDs with continuous profiles, These are clearly visible in the branched spines in Figure 2C (IV) as continuous PSDs.

Perforated PSDs are defined in the present study as those that contain one discontinuous PSD profile in serial sections, while segmented synapses (as described by Geinisman et al., 1992a) are those containing two or more discontinuous PSD profiles, as shown in the series of thin sections in Figure 3A. The five electron micrographs in Figure 3A (labeled 17–21) are part of a series of 140 serial sections of a large spine (mushroom shaped), contacted by a synapse with a segmented PSD. The 3D reconstruction from the 140 sections is shown in Figure 3B, with the segmented PSD indicated by arrows. A macular synapse is formed on a thin spine adjacent to the mushroom spine and is also present in the thin section in Figure 3A (labeled 17). Figure 3C shows a thin section from a separate area of the molecular layer

of the dentate with an axodendritic synapse (shaft synapse), and below it an unperforated (macular) synapse on a stubby spine.

The perforated synapses (both simple perforated and segmented), as a percentage of the total number of synapses, comprised 82% in the stimulated hemisphere of rats that sustained potentiation and 44% in the control hemisphere. For rats that did not sustain potentiation, the percentage of perforated synapses was 42% in the stimulated hemisphere and 60% in the unstimulated hemisphere. These data were analyzed in terms of the differences in perforated or segmented synapse in rats in which LTP was sustained and in the second group that did not sustain LTP (Fig. 4).

There is a significant increase ($P < 0.01$) in the percentage of perforated segmented synapses in the stimulated hemisphere of rats that sustained potentiation compared to the control (unstimulated) hemisphere (Fig. 4), but there are no significant differences in the percentage of segmented synapses between hemispheres of the rats that failed to sustain potentiation (Fig. 4). Nor were there any significant differences between the proportions of simple perforated synapses (those with a single perforation) in the stimulated hemisphere of rats that sustained LTP compared with the control (unstimulated) hemisphere, nor between hemispheres of rats that failed to sustain LTP.

DISCUSSION

The primary objective of this study was to determine spine and synapse density parameters in rats that could sustain LTP and compare the data with those from aged rats that were stimulated but that failed to sustain LTP. In the present case, 45 min after high-frequency stimulation of the perforant path, one-half of a group of aged (22 month old) rats exhibited LTP whilst the other half failed to show LTP. The level of LTP sustained in the aged group was similar to that of a group of 4-month-old rats (all of which sustained LTP after 45 min).

While synapse density was estimated in the present study using unbiased stereological techniques at the electron microscopic level, dendritic spine density was assessed from Golgi-impregnated sections. One criticism of the Golgi technique is that silver impregnation may not always fill all spines. Our estimates for visible spine density (from 0.95 to 1.13/μm from the stimulated hemispheres) are within the same range as we found previously (Rusakov et al., 1997). Although we cannot rule out that this is an underestimation, these values, corrected by the stereological factor (1.62), are actually higher than the longitudinal spine density (1.0/μm) reported by Trommald et al. (1996) using electron microscopic examination of serial sections from granule cell dendrites. In any case, our conclusions are based on comparison between samples of data (control vs test) obtained in a similar way, and the likelihood that these samples might have inherently differential biases during Golgi impregnation is small. The Golgi technique has a major advantage, however, in that it allows one to observe and analyze, in each animal, a large number of dendritic fragments and, correspondingly, thousands of dendritic spines belonging to different cells from the population of interest. Only very detailed 3D reconstruction methods (e.g., Sorra and Harris, 1998, 2000; Fiala et al., 2002; see also Fig. 2C) would allow precise morphometric reconstruction of spines and the synapses they accommodate, but at the expense of time permitting only a limited number of constructions.

Previous studies reported several types of transformations in dendritic spines and synapses during the first hour of LTP induction, ranging from growth to collapse, and elongation to shortening and these dynamic morphological activities take place rapidly (Smart and Halpain, 2000). An increase in spine density was observed 30 min after LTP induction in young rats (Trommald et al., 1996). In contrast, serial section EM studies by Harris et al.

(1992) showed no significant changes in synapse density in the CA1 region, and Desmond and Levy (1986, 1990) concluded that there was no change in spine density in the dentate gyrus after LTP induction. In an in vitro study at 2 h poststimulation, Sorra and Harris (1998) observed no change in synapse density and suggested the occurrence of synapse stability at this time poststimulation.

In the present study, 45 min after acute high-frequency stimulation in vivo, no significant changes in dendritic spine density or length, or in synapse density, were observed in the dentate gyrus of potentiated rats. While our data also indicate a stability in synapse numbers, more subtle changes in existing synapses occur, notably the formation of segmented perforated synapses that have multiple completely partitioned transmission zones. The percentage of these increased significantly, by two- to threefold, in the stimulated dentate gyrus of aged potentiated rats compared with both the unstimulated hemisphere and stimulated but nonpotentiated aged rats (i.e., rats that did not sustain LTP). These data support those of Geinisman et al. (1992b, 1993), which showed that induction of LTP in aged rats is followed by a selective increase only in the number of perforated axospinous synapses that exhibit a PSD consisting of separate segments (segmented PSDs), which we analyzed. However, there was a marked difference in the stimulation protocol used to induce LTP in the present study compared to that of Geinisman et al. (1992b, 1993); in the latter, chronically implanted rats received daily stimulation for 4 days; it can be concluded that the increase in segmented synapses represents a persistent change. The findings in the present study indicate that this change occurs rapidly. From a functional point of view, perforated synapses might play a role in increasing synaptic strength by expressing larger PSDs and perhaps accommodating expression of additional receptors (Malenka and Nicoll, 1999). In addition, the PSDs in segmented synapses are separated by transmission zones and have corresponding presynaptic boutons (Harris and Stevens, 1989; Harris and Kater, 1994). One possible conclusion that can be drawn from our data is that the ability of aged rats to sustain LTP is dependent on the formation of segmented perforated synapses or axospinous synapses with multiple transmission zones for the same presynaptic bouton. However, it may not simply be a case that larger PSDs express more receptors. If one examines models of neurotransmitter release, it appears that two distinct active zones in close spatial approximation to each other are actually more efficient than a single isolated active zone of equivalent area (Cooper et. al., 1996). Thus formation of synapses with segmented perforations may owe more to increasing synaptic efficacy than formation of new synapses via splitting of preexisting spines (Fiala et al., 2002).

A number of previous studies have found an increase in the number of branched spines and perforated synapses after LTP induction (Geinisman et al., 1991, 1992b, 1993; Buchs and Muller, 1996; Toni et al., 1999), and a remodeling of synaptic membranes (Toni et al., 2001). Branched or bifurcating spines are a subset of spines that divide the stem into two branches at variable points from the origin (Sorra and Harris, 1998). In most cases, the branched spines terminate into an active zone containing both postsynaptic densities from the same presynaptic bouton. Moser et al. (1994), Trommald et al. (1996), and Rusakov et al. (1995) have shown that learning and LTP are associated with an increase in the proportion of branched spines; one of the most striking results is the direct observation by Engert and Bonhoeffer (1999), using two-photon confocal microscopy of the formation of new spines 30–60 min after application of an LTP-inducing protocol, a mechanism that requires NMDA receptor activation. Using precise 3D electron microscopic reconstruction of spines and synapses, Fiala et al. (2002) cast doubt on these data, by showing that spines do not split during LTP. However, Fiala et al. (2002) carried out their studies 2 h poststimulation in vitro on acute hippocampal slices, although they also examined the possibility of spine splitting during maturation by examining multiple synapse boutons from perfusion-fixed rat hippocampus at day 21 postnatal and in mature rats. This showed no

difference in bouton number between the two ages, suggesting strongly that spine splitting did not occur even during maturation. In contrast, our study has shown that a small proportion of spines in the dentate gyrus do branch significantly 45 min after potentiation induced by high-frequency stimulation in vivo. However, branched spines were also found to increase in the stimulated but nonpotentiated rats, so it would appear that even if one accepts that spine branching occurs, they do not represent functional synapses at this time point and are not necessarily a requirement for LTP per se. This raises the possibility that the de novo branched spines could indeed disappear at a later time in animals that do not sustain LTP. In contrast, it may indicate that LTP requires both pre- and postsynaptic processes, but that in the nonpotentiated rats only part of that process has occurred and without the presynaptic element (in this case, the formation of segmented perforated synapses), LTP is not sustained. Geinisman et al. (1989) suggested that perforated synapses on double-headed dendritic spines might be a possible substrate of synaptic plasticity. The present data would imply that it is the combination of perforation and splitting of spines, not splitting per se, which is the indicator of sustained synaptic plasticity after LTP induction.

Acknowledgments

This work was supported by BBSRC grant 108/BI 11211, by Leverhulme Trust grant F00269G (to V.I.P.), and by RFBR grant 02-04-48890a.

Grant sponsor: Biological and Biotechnology Research Council (BBSRC) Grant number: 108/BI 11211; Grant sponsor: Leverhulme Trust Grant number: F00269Gm Grant sponsor: Russian Foundation for Basic Research (RFBR) Grant number: 02-04-48890a.

REFERENCES

Abraham WC, Logan B, Greenwood JM, Dragunow M. Induction and experience dependent consolidation of stable long-term potentiation lasting months in the hippocampus. J Neurosci. 2002; 22:9626–9634. [PubMed: 12417688]

Barnes CA, Rao G, Houston FP. LTP induction threshold change in old rats at the perforant path-granule cell synapse. Neurobiol Aging. 2000; 21:613–620. [PubMed: 11016529]

Bliss TVP, Lomo T. Long-lasting potentiation of synaptic transmission in the dentate area of the anaesthetized rabbit following stimulation of the perforant path. J. Physiol (Lond). 1973; 232:331–356. [PubMed: 4727084]

Bliss TVP, Collingridge GL. A synaptic model of memory: long-term potentiation in the hippocampus. Nature. 1993; 361:31–39. [PubMed: 8421494]

Bozon B, Davis S, Laroche S. Regulated transcription of the immediate-early gene Zif268: mechanisms and gene dosage-dependent function in synaptic plasticity and memory formation. Hippocampus. 2002; 12:570–577. [PubMed: 12440572]

Buchs PA, Muller D. Induction of long-term potentiation is associated with major ultrastructural changes of activated synapses. Proc Natl Acad Sci USA. 1996; 93:8040–8045. [PubMed: 8755599]

Chang FL, Greenough WT. Transient and enduring morphological correlates of synaptic activity and efficacy change in the rat hippocampal slice. Brain Res. 1984; 309:35–46. [PubMed: 6488013]

Cooper RL, Winslow JL, Govind CK, Atwood HL. Synaptic structural complexity as a factor enhancing probability of calcium mediated transmitter release. J Neurophys. 1996; 75:2451–2466.

deToledo-Morrell L, Geinisman Y, Morrell F. Age-dependent alterations in hippocampal synaptic plasticity: relation to memory disorders. Neurobiol Aging. 1988; 9:581–590. [PubMed: 3062469]

Desmond N, Levy W. Changes in the numerical density of synaptic contacts with long-term potentiation in the hippocampal dentate gyrus. J Comp Neurol. 1986; 253:466–475. [PubMed: 3025272]

Desmond NL, Levy WB. Synaptic interface surface area increases with long-term potentiation in the hippocampal dentate gyrus. Brain Res. 1988; 453:308–314. [PubMed: 3401768]

Desmond N, Levy W. Morphological correlates of long-term potentiation imply the modification of existing synapses, not synapto-genesis, in the hippocampal dentate gyrus. Synapse. 1990; 5:139–143. [PubMed: 2309158]

Engert F, Bonhoeffer T. Dendritic spine changes associated with hippocampal long-term synaptic plasticity. Nature. 1999; 399:66–70. [PubMed: 10331391]

Fairen A, Peters A, Saldanha J. A new procedure for examining Golgi impregnated neurons by light and electron microscopy. J Neurocytol. 1977; 6:311–337. [PubMed: 71343]

Fiala JC, Allwardt B, Harris KM. Dendritic spines do not split during hippocampal LTP or maturation. Nature Neurosci. 2002; 5:297–298. [PubMed: 11896399]

Geinisman Y, Morell F, deToledo-Morrell L. Perforated synapses on double-headed dendritic spines: a possible substrate of synaptic plasticity. Brain Res. 1989; 480:326–329. [PubMed: 2713659]

Geinisman Y, deToledo-Morrell L, Morrell F. Induction of long-term potentiation is associated with an increase in the number of axospinous synapses with segmented postsynaptic densities. Brain Res. 1991; 566:77–88. [PubMed: 1814558]

Geinisman Y, Morrell F, deToledo-Morrell L. Increase in the number of axospinous synapses with segmented post-synaptic densities following hippocampal kindling. Brain Res. 1992a; 569:341–347. [PubMed: 1540834]

Geinisman Y, deToledo-Morrell L, Persina IS, Rossi M. Structural synaptic plasticity associated with the induction of long-term potentiation is preserved in the dentate gyrus of aged rats. Hippocampus. 1992b; 2:445–456. [PubMed: 1308201]

Geinisman Y, deToledo-Morrell L, Morrell F, Heller R, Rossi M, Parshall R. Structural synaptic correlate of long-term potentiation: formation of axospinous synapses with multiple, completely partitioned transmission zones. Hippocampus. 1993; 3:435–446. [PubMed: 8269035]

Geinisman Y, deToledo-Morrell L, Morrell F. Comparison of structural synaptic modifications induced by long-term potentiationin the hippocampal dentate gyrus of young adult and aged rats. Ann NY Acad Sci. 1994; 747:452–466. [PubMed: 7847690]

Geinisman Y, deToledo-Morrell L, Morrell F, Persina IS, Beatty MA. Synapse restructuring associated with the maintenance phase of hippocampal long-term potentiation. J Comp Neurol. 1996; 368:413–423. [PubMed: 8725348]

Goldin M, Segal M, Avignone E. Functional plasticity triggers formation and pruning of dendritic spines in cultured hippocampal networks. J Neurosci. 2001; 21:186–193. [PubMed: 11150335]

Gundersen H. Stereology of arbitary particles. A review of unbiased number and size estimators and the presentation of some new ones in memory of William R. Thompson. J Microsc (Lond). 1986; 143:3–45.

Harris KM, Stevens JK. Dendritic spines of CA1 pyramidal cells in the rat hippocampus: serial electron microscopy with reference to their biophysical characteristics. J Neurosci. 1989; 9:2982–2997. [PubMed: 2769375]

Harris K, Kater S. Dendritic spines: cellular specializations imparting both stability and flexibility to synaptic function. Annu Rev Neurosci. 1994; 17:341–371. [PubMed: 8210179]

Harris KM, Jensen FE, Tsao B. Three-dimensional structure of dendritic spines and synapses in rat hippocampus (CA1) at postnatal day 15 and adult ages: implications for the maturation of synaptic physiology and long-term potentiation. J Neurosci. 1992; 12:2685–2705. [PubMed: 1613552]

Hosokawa T, Rusakov DA, Bliss TV, Fine AF. Repeated confocal imaging of individual dendritic spines in the living hippocampal slice: evidence for changes in length and orientation associated with chemically induced LTP. J Neurosci. 1995; 15:5560–5573. [PubMed: 7643201]

Korkotian E, Segal M. Spike-associated fast contraction of dendritic spines in cultured hippocampal neurons. Neuron. 2001; 30:751–758. [PubMed: 11430808]

Malenka RC, Nicoll RA. Long-term potentiation—a decade of progress? Science. 1999; 285:1870–1874. [PubMed: 10489359]

Maletic-Savatic M, Malinow R, Svoboda K. Rapid dendritic morphogenesis in CA1 hippocampal dendrites induced by synaptic activation. Science. 1999; 283:1870–1874.

McGahon B, Lynch M. The synergism between metabotropic glutamate receptor activation and arachidonic acid in the rat hippocampus. NeuroReport. 1996; 5:2353–2357. [PubMed: 7881058]

Moser MB, Trommald M, Andersen P. An increase in dendritic spine density on hippocampal CA1 pyramidal cells following spatial learning in adult rats suggests the formation of new synapses. Proc Natl Acad Sci USA. 1994; 91:12673–12675. [PubMed: 7809099]

Moser EI, Krobert KA, Moser MB, Morris RG. Impaired spatial learning after saturation of long-term potentiation. Science. 1998; 281:2038–2042. [PubMed: 9748165]

Muller D, Toni N, Buchs PA. Spine changes associated with long-term potentiation. Hippocampus. 2000; 10:596–604. [PubMed: 11075830]

Murase S, Mosser E, Schuman EM. Depolarization drives beta-catenin into neuronal spines promoting changes in synaptic structure and function. Neuron. 2002; 35:91–105. [PubMed: 12123611]

Nimchinsky EA, Sabatini BL, Svoboda K. Structure and function of dendritic spines. Annu Rev Physiol. 2002; 64:313–353. [PubMed: 11826272]

Patel S, Stewart MG. Changes in the number and structure of dendritic spines 25 hours after passive avoidance training in the domestic chick, *Gallus domesticus*. Brain Res. 1988; 449:34–46. [PubMed: 3395852]

Rusakov D, Stewart MG, Sojka M, Richter-Levin G, Bliss TV. Dendritic spines form “collars” in hippocampal granule cells. NeuroReport. 1995; 6:1557–1561. [PubMed: 7579148]

Rusakov D, Richter-Levin G, Stewart MG, Bliss TV. Reduction in spine density associated with long-term potentiation in the dentate gyrus suggests a spine fusion-and-branching model of potentiation. Hippocampus. 1997; 7:489–500. [PubMed: 9347346]

Smart FM, Halpain S. Regulation of dendritic spine stability. Hippocampus. 2000; 10:542–554. [PubMed: 11075824]

Sorra K, Harris K. Stability in synapse number and size at 2 hr after long-term potentiation in hippocampal area CA1. J Neurosci. 1998; 18:658–671. [PubMed: 9425008]

Sorra KE, Harris KM. Overview on the structure, composition, function, development, and plasticity of hippocampal dendritic spines. Hippocampus. 2000; 10:501–511. [PubMed: 11075821]

Stephan A, Davis S, Salin H, Dumas S, Mallet J, Laroche S. Age-dependent differential regulation of genes encoding APP and alpha-synuclein in hippocampal synaptic plasticity. Hippocampus. 2002; 12:55–62. [PubMed: 11918289]

Sterio D. The unbiased estimation of number and sizes of arbitary particles using the disector. J Microsc. 1984; 134:127–136. [PubMed: 6737468]

Steward O, Vinsant SL. The process of reinnervation in the dentate gyrus of the adult rat: A quantitative electron microscopic analysis of terminal proliferation and reactive synaptogenesis. J Comp Neurol. 1983; 214:370–386.

Stewart MG, Harrison E, Rusakov DA, Richter-Levin G, Maroun M. Re-structuring of synapses 24 hours after induction of long-term potentiation in the dentate gyrus of the rat hippocampus in vivo. Neuroscience. 2000; 100:221–227. [PubMed: 11008162]

Toni N, Buchs P, Nikonenko I, Bron CR, Muller D. LTP promotes formation of multiple spine synapses between a single axon terminal and a dendrite. Nature. 1999; 402:421–425. [PubMed: 10586883]

Toni N, Buchs PA, Nikonenko I, Povilaitite P, Parisi L, Muller D. Remodeling of synaptic membranes after induction of long-term potentiation. J Neurosci. 2001; 21:6245–6251. [PubMed: 11487647]

Trommald M, Hulleberg G, Andersen P. Long-term potentiation is associated with new excitatory spine synapses on rat dentate granule cells. Learn Mem. 1996; 2/3:218–228. [PubMed: 10456092]

Tsvetkov E, Carlezon WA, Benes FM, Kandel ER, Bolshakov VY. Fear conditioning occludes LTP-induced presynaptic enhancement of synaptic transmission in the cortical pathway to the lateral amygdala. Neuron. 2002; 34:289–300. [PubMed: 11970870]

Weeks AC, Ivanco TL, Leboutillier JC, Racine RJ, Petit TL. Sequential changes in the synaptic structural profile following long-term potentiation in the rat dentate gyrus. II. Induction/early maintenance phase. Synapse. 2000; 36:286–296. [PubMed: 10819906]

Weeks AC, Ivanco TL, Leboutillier JC, Racine RJ, Petit TL. Sequential changes in the synaptic structural profile following long-term potentiation in the rat dentate gyrus. III. Long-term maintenance phase. Synapse. 2001; 40:74–84. [PubMed: 11170224]

Weeks AC, Ivanco TL, Leboutillier JC, Marrone DF, Racine RJ, Petit TL. Unique changes in synaptic morphology following tetanization under pharmacological blockade. Synapse. 2003; 47:77–86. [PubMed: 12422376]

Xu L, Anwyl R, Rowan MJ. Spatial exploration induces a persistent reversal of long-term potentiation in rat hippocampus. Nature. 1998; 394:891–894. [PubMed: 9732871]

Europe PMC Funders Author Manuscripts

Europe PMC Funders Author Manuscripts

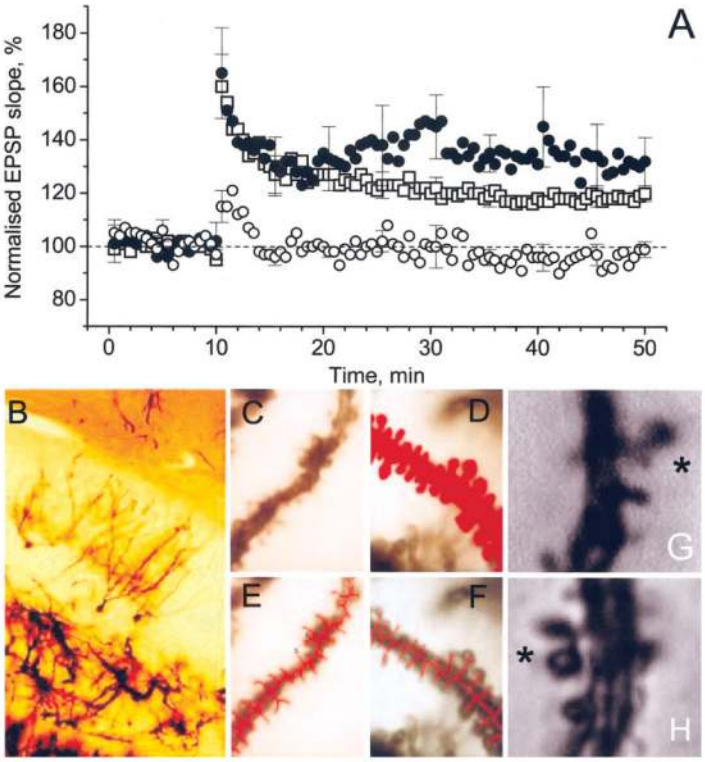

FIGURE 1.

Quantification of dendritic spine populations. Representative excitatory postsynaptic potential (EPSP) slopes (percentage) of aged rats that sustained long-term potentiation (LTP) (●) and rats that did not sustain LTP (◯), during the course of the experiment. For comparison, EPSPs of six young (4-month-old) rats that sustained LTP are shown (□). B: Golgi-impregnated section from the dentate gyrus of an aged rat showing three granule cells with dendritic arborizations. C, E: One dendritic fragment as an original image (C) and one with a superimposed skeleton (E). D, F: Another dendritic fragment with the generated profile image (D) and an overlap of the original and skeletonized image (F) G: Short segment of Golgi impregnated dendrite at high magnification showing simple and branched spines (*), and H shows more clearly a branched spine (*). B, × 40; C–F, × 200;G&H, × 1000. [Color figure can be viewed in the online issue, which is available at www.interscience.wiley.com].

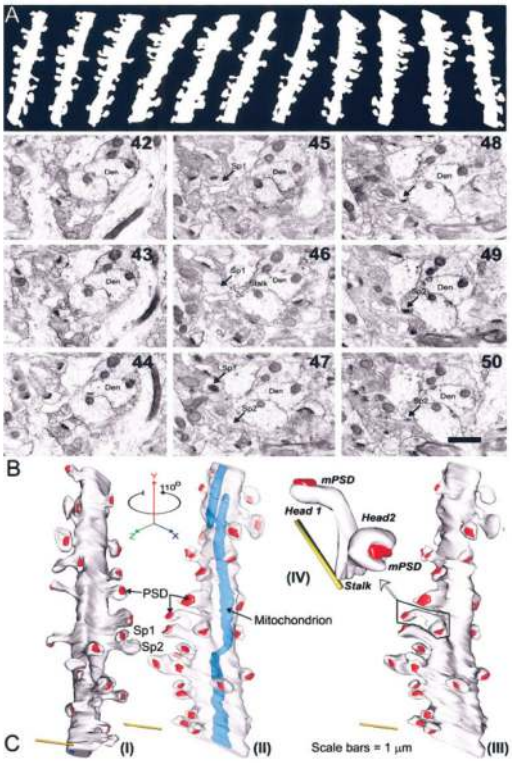

FIGURE 2.

A–C: To determine whether our counts in Golgi preparations were compatible with the precise data that can be provided from 3D reconstructions of serial ultrathin sections, a dendritic segment was reconstructed from the middle molecular layer of the dentate gyrus, ~100 μm from the granule cell layer. A series of 150 sections was prepared and the dendritic segment (reconstructed with software from Dr. J. Fiala and Dr. K. Harris: http://synapses.bu.edu), is shown in A at different rotational angles. Nine of the 150 ultrathin sections used to prepare the reconstruction are shown in B (section numbers 42–50). A dendrite (den) can be seen in each section; two spines (Sp1 and Sp2) are indicated by the small arrow in sections 45–50, a spine stalk is evident in section 46. C: The reconstructed segment (I)) contains 30 spines. B: The two spines (Sp1 and Sp2) are actually a single spine with two branches, each contacted by a postsynaptic density (PSD), indicated by the red color. The two separate branches (Sp1 and Sp 2) comprise 6.7% of the total spines in the segment. Mitochondria are present in the electron micrographs (B) as separate entities but are actually a single elongated filamentous structure as seen in blue in 2C (II). To make a visual comparison with the typical profile images of dendrites of the same order seen in Golgi preparations, the reconstructed segment was rotated along its longitudinal axis and its profile image recorded at each rotation angle. These profiles (C) appear consistent with the Golgi profiles shown in Fig. 1C–F. An example of bifurcating spines (Sp1 and Sp2) in C (I) is outlined in C (III) and is shown at high magnification in C (IV) with two separate heads and a common stalk. Scale bar = 1 μm in B. [Color figure can be viewed in the online issue, which is available at www.interscience.wiley.com].

Europe PMC Funders Author Manuscripts

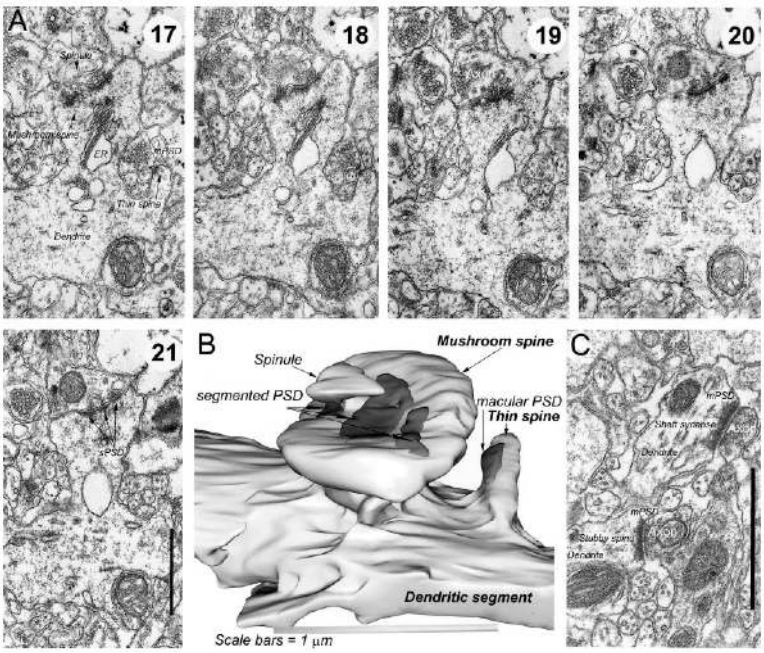

FIGURE 3.

A: Five electron micrographs from the middle molecular layer of the hippocampus (labeled 17–21), which are part of a series of 140 sections of a large spine (mushroom shaped), contacted by a synapse with a segmented postsynaptic density (PSD) (i.e., with a discontinuous PSD profile). No. 17, a spinule, is shown in the synaptic bouton above the segmented PSD, and endoplasmic reticulum (ER) is visible in the spine forming a spine apparatus. A thin spine is on the right of the micrograph with a macular PSD (mPSD). The presynaptic bouton is more clearly visible in A (19), where it is labeled as axon terminal (axon) and the segmented PSD is labeled in A (21). B: A 3D reconstruction from the 140, with the segmented PSD indicated by arrows. A macular synapse that was present in the thin section in A (17), is formed on a thin spine adjacent to the mushroom spine. C: A thin section from a separate area of the molecular layer of the dentate with an axodendritic synapse (shaft synapse), which has a macular PSD (mPSD), and below it an unperforated mPSD on a stubby spine. Scale bar = 1 μm in A–C.

Europe PMC Funders Author Manuscripts

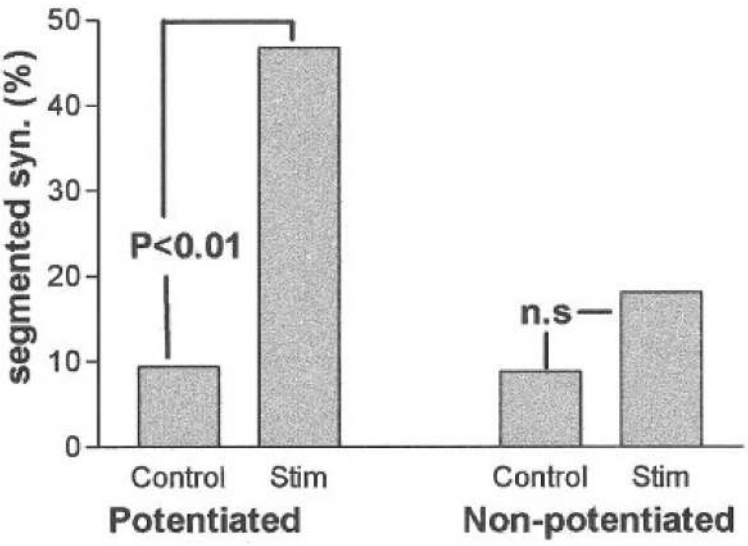

FIGURE 4.

Relative percentage changes in segmented perforated synapses (segmented as described in Fig. 3) in the middle molecular layer of the dentate gyrus of aged rats. There are significant differences between control and stimulated hemispheres in rats that sustained long-term potentiation (LTP) (potentiated) ($P < 0.01$), but not between hemispheres of rats that did not sustain LTP (nonpotentiated).

Europe PMC Funders Author Manuscripts

Europe PMC Funders Author Manuscripts

TABLE 1

Morphometric Parameters of Dendritic Spines and Synapses*

	Aged potentiated rats		Aged nonpotentiated rats	
	Left hemisphere (control)	**Right hemisphere (stimulated)**	**Left hemisphere (control)**	**Right hemisphere (stimulated)**
Spine density (μm^{-1})[c]	0.96 ± 0.09	0.95 ± 0.12	1.26 ± 0.07	1.13 ± 0.08
Spine length (μm)	1.04 ± 0.11	0.94 ± 0.08	0.95 ± 0.04	0.81 ± 0.02
Branched spines (%)	3.94 ± 0.41	6.58 ± 0.64	2.53 ± 0.22	6.37 ± 0.26
Spine synapses (μm^{-3})	1.67 ± 0.32	1.32 ± 0.06	1.48 ± 0.23	1.24 ± 0.06
Shaft synapses (μm^{-3})	0.29 ± 0.08	0.57 ± 0.23	0.26 ± 0.05	0.20 ± 0.06
Total synapses (μm^{-3})	2.01 ± 0.37	1.49 ± 0.07	1.79 ± 0.06	1.46 ± 0.06

LTP, long-term potentiation; N_{Vsyn}, synapse density (the number of synapses that appear in the counting frame of one slice (the reference).

*Summary of spine density (number per μm), spine length (μm), branched spines (as percentage of total spine numbers), spine synaptic density (N_{Vsyn} per μm^3), shaft synapse, density (N_{Vsyn} per μm^3), and total synapse density (N_{Vsyn} per μm^3), in the middle molecular layer of the dentate gyrus of aged (22-mon-old) rats that sustained LTP, and rats that did not sustain LTP, 45 min after initial stimulation.

[a]The right hemisphere was stimulated, while the left was the unstimulated (control) hemisphere.

[b]Data are mean values (n = 4) ±SEM. None of the differences between control and stimulated hemispheres are significant for either those rats that sustained potentiation or those that failed to sustain potentiation.

[c]Spine density values are shown without stereological correction.